Complete Genome Sequence of *Pseudomonas Stutzeri* S116 Provides Insights into the Mechanism of Microbial Fuel Cells

Peng Li (lpqp3818081@163.com)
Zhejiang Ocean University https://orcid.org/0000-0003-0276-4760
Wenfeng Yuan
Zhejiang Ocean University
Yitie Huang
Zhejiang Ocean University
Caiyu Zhang
Zhejiang Ocean University
Chide Ni
Zhejiang Ocean University
Qi Lin
Fisheries Research Institute of Fujian
Zhihuang Zhu
Fisheries research insititute of Fujian
Jianxin Wang
Zhejiang Ocean University

Research Article

Keywords: biocatalyst, microbial fuel cells, Pseudomonas stutzeri, complete genome

Posted Date: January 14th, 2022

DOI: https://doi.org/10.21203/rs.3.rs-1215240/v1

Abstract

To identify suitable biocatalysts applied in microbial fuel cells (MFCs), *Pseudomonas stutzeri* S116 isolated from marine sludge was investigated, which possessed excellcent bioelectricity generation ability (BGA). Herein, *P. stutzeri* as a bioanode and biocathode achieved maximum output voltage (254.2 mV and 226.0 mV), and power density of (765 mW/m^2 and 656.6 mW/m^2). Complete genome sequencing of *P. stutzeri* was performed to reveal its potential microbial functions. The results exhibited that the strain was the ecologically dominant *Pseudomonas*, and its primary annotations were associated with energy production and conversion (6.84%), amino acid transport and metabolism (6.82%) and inorganic ion transport and metabolism (6.77%). The thirty-six genes involved in oxidative phosphorylation indicate that strain possesses an integrated electron transport chain. Moreover, many genes encoding redox mediators (mainly riboflavin and phenazine) were detected in the databases. Simultaneously, thiosulfate oxidization and dissimilatory nitrate reduction were annotated in the sulfur metabolism and nitrogen metabolism pathway. Gene function and cyclic voltammetry (CV) analysis indicated BGA of *P. stutzeri* probably was attributed to its cytochrome *c* and redox mediators, which enhance extracellular electron transfer (EET) rate.

Key Points

- *Pseudomonas stutzeri* S116 *oxidizes thiosulfate to generate bioelectricity.*
- *Genes encoding riboflavin and phenazine were detected simultaneously.*
- *Metabolic pathways involved in electricity generation for MFCs was predicted.*

Introduction

Sulfur-oxidizing bacteria (SOB) can oxidize sulfur compounds as energy sources and utilize inorganic carbon (CO_2) for their growth (Kelly et al. 1997). Therefore, they play an important role in environmental remediation, which can remove pollutants containing reduced sulfide and fix CO_2 (Pokorna et al. 2015). Previously reported SOB mainly belong to the genera *Thiomonas*, *Acidithiobacillus*, *Thiothrix*, *Pseudomonas*, *Thiobacillus*, *Halothiobacillus*, *Chlorobium*, *Rhodospirillum* and *Sulfurimonas* (Zhou et al. 2015; Omri et al. 2013; Quijano et al. 2018; San et al. 2019). Current studies focused on metal recovery from minerals (Mubaroka et al. 2017), removal of high concentrations of H_2S (Wu et al. 2020; Prenafeta et al. 2014), and wastewater treatment containing reduced sulfur compounds (S^{2-}, $S_2O_3^{2-}$, S) (Sedky et al. 2019). However, few studies have reported SOB applied in MFCs, the related mechanisms of its bioelectricity generation have rarely been investigated.

MFCs are a promising technology for treating wastewater and pollutants, which can directly convert chemical energy into electrical energy via electrogenic microorganisms (Samsudeen et al. 2016; Marshall et al. 2013). The large-scale application of MFCs is limited due to electrode materials and

electrochemically active bacteria (EAB) (Xie et al. 2012). Compared with costly materials, screening microorganisms with excellent electrocatalytic activity is more practical and inexpensive for enhancing MFC performance. As a significant member of EAB, *Pseudomonas* was verified it can directly or indirectly transfer electrons to an anode electrode (Kumar et al. 2016; Bosire et al. 2016; Xi et al. 2019).

Generally, the mechanism of electricity generation in MFCs is as follows: Electroactive microorganisms in the anodic chamber oxidize substrates (pollutants or organic substances) to generate electrons, subsequently, the electrons are carried by an external electric circuit to a cathode, finally, current flows and electrical energy generates (Chadwick et al. 2019; Cao et al. 2019). Clearly, EET efficiency definitely affects MFC performance as an essential factor. Current studies provide three basic mechanisms of EET: 1. c-type cytochromes. Cytochromes can transfer electrons from the cell metabolism to outside of the cell (Li et al. 2018; Logan et al. 2019). 2. Nanowires. Specific pili plays an important role in EET (Logan et al. 2009; Saratale et al. 2017). 3. Redox mediators. Mediators (such as riboflavin) can promote electron transfer from electroactive bacteria to anodes in MFCs (Xu et al. 2016).

Pseudomonas successfully applied in MFCs is attributed to its excellent biodegradation capability (Ali et al. 2017; Zhang et al. 2019; Boobalan et al. 2019; Saranya et al. 2018; Hwang et al. 2019). However, the mechanism underlying electricity generation in biocathode MFCs has rarely been reported. Currently, biocathode MFCs have attracted more and more attentions as the promising technology applied in energy recovery. Biocathode is mainly classified as follows: (1) Oxygen. Due to the low-cost and high redox potential, oxygen is considered as an excellent terminal electron acceptor. Cathodic bacteria can reduce oxygen to generate electricity (Clauwaert et al. 2007). (2) Inorganic salts. nitrate and sulfate directly accept electrons via microbial metabolism (denitrifying bacteria and sulfate reducting bacteria) (Holmes et al. 2004). (3) Others. Fumarate, urea, carbon dioxide and redox mediators can be used as electron acceptors (Park et al. 1999).

Based on the striking bifunctional biocatalysis of *P. stutzeri* S116, CV and electrochemical impedance spectroscopy (EIS) method were performed to investigate its electrochemical activity, complete genome sequencing was used to determine its genetic functions, which partly interpret the mechanism of bioanodic and biocathodic catalysis in MFCs.

Materials And Methods

Sample preparation and strain screening

Marine activated sludge samples were collected from a marine sewage treatment plant. 50 mL of sludge sample was suspended in 450 mL of sterile seawater, then mixed with a dilution ratio of 10^{-1}. The mixture was stored at 4 °C for enrichment and isolation. 1 L of the enrichment culture medium for SOB (ECMS) contained the following components: 1 L sterile seawater, 10 g $Na_2S_2O_3{\cdot}5H_2O$, 4.0 g KH_2PO_4, 4.0 g K_2HPO_4, 0.8 g MgSO4·$7H_2O$, 0.4 g NH_4Cl, and 10 mL of trace elements. 1 L trace element solution contained 50.0 g EDTA, 22.0 g $ZnSO_4{\cdot}7H_2O$, 5.54 g $CaCl_2$, 5.06 g $MnCl_2{\cdot}4H_2O$, 4.99 g $FeSO_4{\cdot}7H_2O$, 1.10 g

$(NH_4)_2MoO_4 \cdot 4H_2O$, 1.57 g $CuSO_4 \cdot 5H_2O$, 1.61 g $CoCl_2 \cdot 6H_2O$, 1 L sterile seawater. Agar (1.5-2%) added as a solidifying agent was used to screen SOB.

A 5 mL aliquot of the prepared sample was inoculated into flasks containing 45 mL of ECMS medium and cultivated at 35 °C with a rotation speed of 120 r/min for 3 days. After three successive cultures, 0.1 mL of the enrichment samples were spread onto agar ECMS plates and incubated at 35 °C for 3 days. Subsequently, colonies were picked and streaked onto fresh agar ECMS plates three times, and purified isolates were obtained.

MFC configuration

A double chamber MFC was configured with two cylindrical glasses. The chambers were separated by a cation exchange membrane Nafion117 (5 cm×5 cm, DuPont, USA). Each chamber had a volume of 100 mL. Reactor 1: The anode and cathode electrode was assembled from a carbon cloth (1.5 cm×1 cm Hesen HCP330N, Shanghai, China), the strain S116 was inoculated in the anodic medium with a volume of 80 mL, 1 L anodic medium contained 0.0352 g KH_2PO_4, 0.128 g NaCl, 0.01 g $FeSO_4 \cdot 7H_2O$, 0.188 g $(NH_4)_2SO_4$, 0.2 g $NaHCO_3$, 0.18 g MgSO4·$7H_2O$, 0.05 g $CaCl_2$, 0.73 g KNO_3, 5 g NaS_2O_3, and 1L artificial seawater. Potassium ferricyanide (50 mM, 80 mL) was used as the catholyte. Reactor 2: The carbon cloth electrodes were equipped in the MFC. Anaerobic activated sludge from a marine sewage treatment plant (Zhoushan, China) was used as the anodic inoculum. Before running the reaction, the anode chamber was filled with 40 mL of sludge and 40 mL of artificial sewage. 1 L artificial sewage contained 0.8787 g CH_3COONa, 0.361 g KNO_3, 0.0255 g KH_2PO_4, 0.0427 g $K_2HPO_4 \cdot 3H_2O$, 1L artificial seawater and 1 mL of trace elements at pH 7.0, the cathodic medium is as same as the anodic medium in Reactor 1. The anode and cathode electrodes were connected by an external copper wire with a 900 Ω resistance. The MFC was operated at 25 °C. All experimental reactions were performed in triplicate to ensure reproducibility.

MFC performance analysis

The output voltage of the MFC was recorded by a data acquisition system. Polarization curves and power density curves were calculated by Ohm's law, which was obtained by changing external resistors. Ohm's law was described as follows: I (A/m^2) =U/(RA) and P (W/m^2) =U^2/(RA), where I is the current density, R is the resistance, P is the power density, U is the voltage, and A is the area of the cathode (Wu et al. 2016).

Cyclic voltammetry (CV) measurement of electrodes were operated by the three-electrode system using an electrochemical workstation (Bio-Logic, SP-300, France). The carbon cloth, platinum electrode and saturated calomel electrode were used as the working, reference and counter electrodes, respectively. CV was performed at a scanning speed of 50 mV/s from -1 to 1.0 V in Reactor 1 (-1 to 0.2 V in Reactor 2). EIS was carried out at a sinusoidal perturbation amplitude of 5 mV in a frequency range from 100 kHz to 5 mHz.

Identification of bacterial species

The purified strain was identified using 16S rRNA gene sequencing. The DNA was extracted by a bacterial genome DNA extraction kit (Ezup, Sangon Biotech, Shanghai), and the 16S rRNA gene was amplified by PCR (2720 thermal cycler, Applied Biosystems) with universal primers (7F: 5'-CAGAGTTTGATCCTGGCT-3', 1540R: 5'-AGGAGGTGATCCAGCCGCA -3'). The loop condition of PCR was as follows: predenaturation for 4 min at 94 °C, 30 cycles of denaturation at 94 °C for 45 s, annealing at 55 °C for 45 s, elongation at 72 °C for 60 s, repair extension at 72 °C for 8 min, and termination reaction at 4 °C. PCR products were purified using 1% agarose gel electrophoresis and subjected to Sanger sequencing (Sangon Biotech (Shanghai) Co., Ltd.). The sequencing results were aligned using BLAST, and phylogenetic trees were constructed by MEGA (MEGA version 7.0) to analyze the obtained gene sequences (Herbold et al. 2014).

Complete genome sequence and functional annotation of *P. stutzeri*

High-quality genomic DNA of *P. stutzeri* was extracted using a QIAGEN Genomic tip (Biomarker Technologies Co., Ltd.). The concentration and purity of DNA were detected using a NanoDrop and Qubit (Thermo Scientific, USA), and large segments were filtered using the BluePippin system (Sage Science, USA). A library was prepared using the large segments DNA, Oxford Nanopore Technologies (ONT) Template prep kit (SQK-LSK109) and NEB Next FFPE DNA Repair Mix kit. The high-quality library was sequenced on the ONT PromethION platform, and the raw sequencing data were obtained.

For genome assembly, quality control of the sequencing data was performed by Guppy3.2.6 software to filter low-quality fragments of the reads. The obtained subreads were assembled using Canu v1.5/ wtdbg v2.2 (Koren et al. 2017). For genome component prediction, coding DNA sequences (CDSs) were predicted using Prodiga V2.50 (Hyatt et al. 2010). tRNAs, rRNAs and ncRNAs were predicted using tRNAscan-SE v1.3.1 (Lowe et al. 1997) and Infernal v1.1 (based on RFAM v12.0 database), respectively. For functional annotation, the predicted gene sequences from Prodiga were aligned by BLAST v2.2.29 (Altschul et al. 1997) against the functional databases of Cluster of Orthologous Groups (COG) (Tatusov et al. 2000), Kyoto Encyclopedia of Genes and Genomes (KEGGs) (Kanehisa et al. 2004), Swiss-Prot (Boeckmann et al. 2003), Non-Redundant Protein Database (Nr) and Gene Ontology (GO) (Ashburner et al. 2000), and the results of gene function annotation were obtained. The Nr database contains comprehensive protein sequences and annotation information. GO unifies the gene products of all species in different databases. KEGG annotation of metabolic pathways in *Pseudomonas stutzeri* S116. Nonredundant protein sequences with high quality are manually annotated using the Swiss-Prot database, and the annotation results have corresponding experimental verification with high reliability.

Results

Morphological characteristics of *P. stutzeri*

The morphology of the isolated strain was characterized by scanning electron microscopy (SEM). SEM (Fig. 1a) showed that the strain adhered to the surface of the electrode. The strain was a short rod without spores, its surface was wrinkled, and the pili was observed (Fig. 1b and 1c). The biofilm was surveyed among carbon fibers (Fig. 1d).

16S rRNA molecular identification and general features description

The isolated strain was identified and confirmed by 16S rRNA gene sequencing. Sequence alignment were performed using BLAST. Sequences with similarities greater than 99% were selected to construct phylogenetic trees using MEGA 7.0. The sequence data of *P. stutzeri* S116 are publicly available in the NCBI database (GenBank accession number MZ220459). The phylogenetic tree showed that the 16S rRNA gene sequence of S116 has 99% homology with *Pseudomonas stutzeri* IHBB 9574 and *Pseudomonas stutzeri* (shown in Figure S1). The phylogeny data (including alignments) are available in the Treebase repository (http://purl.org/phylo/treebase/phylows/study/TB2:S28911?x-access-code=52f486836b34e93c0c34658911e7e960&format=html). The general features of S116 was described in Table S1. The strain was deposited in China General Microbiological Culture Collection Center (CGMCC) with the deposit number CGMCC 1.19374.

Electrochemical property of the bioanode and biocathode

Thirty milliliters of the medium was replaced by fresh solution when the output voltage of the MFC decreased to approximately 50 mV. After the MFC was operated for 30 h, the Reactor 2 reached the stable generation voltage in the first cycle with peak voltage at 170.5 mV, and for 80 h the Reactor 1 reached the highest peak voltage at 254.2 mV. During the second and third cycles, the Reactor 1 and 2 reached the highest output voltages of 228.3 mV and 225.5 mV, respectively. It took less than 10 hours for the Reactor 1 to produce an output voltage from the lowest voltage to the highest voltage (Fig. 2a).

To investigate the electrochemical activity of electrogenic microorganism in MFCs, CV analysis of bioanode and biocathode were performed (shown in Fig. 2b and c). The bioelectrode compared with the bare carbon cloth electrode possessed distinct redox peaks in the CV spectra, which indicated that the electrocatalytic activity of *P. stutzeri* S116 was associated with the electrode. The bioanode exhibited two distinct reduction peaks (-0.92 mA at -0.504 V, -0.845 mA at -0.665 V) and the highest oxidative peak current of 0.595 mA at 0.308 V. The biocathode exhibited three distinct oxidation peaks (-0.13 mA at -0.488 V, 0.246 mA at -0.354 V, 0.105 mA at -0.24 V) and reduction peaks (-1.1 mA at -0.795 V, -0.743 mA at -0.62 V, -0.584 mA at -0.52 V). Simultaneously, for bare bioanode, no distinct redox reaction was measured. The position of the redox peak reflects the redox potential of components involved in ETT (Feng et al. 2010). In addition, the size of the redox peak represents the electrochemical activity of *P. stutzeri*.

Polarization and power density curves of the MFCs were tested during the third cycle when the Reactors generated voltage at the highest point (shown in Fig. 3d). The obtained maximum power was 765 mW/m^2 (Reactor 1) and 656.6 mW/m^2 (Reactor 2), respectively.

The interaction between the electrogenic microbe and the electrodes in MFCs was analyzed by EIS. The Nyquist plot (Figure S2) indicated that the bioelectrodes had a similar semicircle diameter, the Rct values in the MFCs were approximately 11.8 Ω (cathode) and 17.0 Ω (anode), respectively, which represented a low charge-transfer resistance (Rct) and rapid electron transfer.

Genomic features of *P. stutzeri* S116

The filtered subreads of the *P. stutzeri* S116 genome were assembled and rectified into a scaffold length of 4,756,665 bp with a GC content of 63.47%. Gene prediction indicated a total gene length of 4,224,096 bp with 4402 CDSs. Noncoding RNA prediction showed that the numbers of rRNAs, tRNAs and ncRNAs were 15, 63, and 76, respectively. Gene annotation in general databases is described as follows: eggNOG (COG) 3842, GO 3371, KEGG 2493, NR 4385, SwissProt 2805. Moreover, CAZy (121), TCDB (1343), and VFDB (887) were annotated in special databases (Fig. 3). Transmembrane protein and secreted protein prediction indicated that the genes were 1111 and 470, respectively. The genome sequence are publicly available in the NCBI database (BioProject accession PRJNA743140, https://www.ncbi.nlm.nih.gov/bioproject/743140/).

Gene function analysis

The protein sequences of genes were aligned against Nr database by BLAST, species distribution was exhibited in Figure S3. 3744 genes are responsible for *Pseudomonas stutzeri* withthe highest proportion (85.38%).

In the COG categories, energy production and conversion (268 genes), amino acid transport and metabolism (267 genes), and inorganic ion transport and metabolism (265 genes) had higher abundances, with proportions of 6.84%, 6.82%, and 6.77%, respectively (shown in Fig. 4). To detect the potential roles of *P. stutzeri*, specific COGs involved in bioelectricity generation were analyzed. Forenergy production and conversion, dehydrogenase (COG0508, COG1012, COG1052, COG1063, COG1071, COG1319, NOG00108, NOG02207), cytochrome c (COG3258, COG2010, COG3909, NOG62129, NOG18013) and electron transport complex (COG2878, COG4657, COG4658, COG4659, COG4660) were the three most abundant gene function class, which are all involved in electron transport (Logan et al., 2010). Simultaneously, the important components of the respiratory chain, such as complex I (NOG31185, NOG34255), Fe-S protein (COG2975, COG3313), NADH dehydrogenase (COG1252), succinate dehydrogenase (COG0479, COG1053), cytochrome b561 (COG3038), and complex III (COG0723, COG1290), were annotated in COGs. Moreover, cytochrome c oxidase (COG2993, COG4736), playing an important component of complex IV, had been annotated, which reduces oxygen to water as the terminal electron acceptor in the respiratory chain (Cai et al., 2020). For amino acid transport and metabolism function, ABC transporter and aminotransferase were relatively higher abundant. With respect to inorganic ion transport and metabolism, ABC transporter, binding-protein-dependent transport systems inner membrane component were two most abundant function.

Genes of *P. stutzeri* were categorized by GO into three functional nodes to determine the biological relevance of the strain: (1) cellular component, which is used to describe subcellular structure, location, and macromolecular complexes; (2) molecular function describes the function of a gene or gene product; (3) biological process describes biological processes of the encoded gene products. Among the three GO categories, biological process was the most abundant (Fig. 5).

In the biological process category, genes involved in metabolic processes (1737 genes) made up the highest proportion (51.5%) of the total genes (3372 genes), cellular process (1497 genes) was 44.4%, single-organism process possessed 38.9% proportion with1312 genes, and localization (536 genes; 15.9%). In the molecular function category, most genes of 1918 were involved in catalytic activity, with a proportion of 56.9%, and in binding, with a proportion of 43.5% (1467 genes). In the cellular component category, 1140 genes was involved in membrane with the highest proportion of 33.8%, membrane part (1040) 30.8%, cell (1030) 30.5%, and cell part (1007) 29.9%.

For *P. stutzeri* S116, the five most abundant genes were annotated in the VFDB (Figure S4), including type IV pili (61 genes), capsule (49 genes), flagella (44 genes), pyoverdine (38 genes) and polar flagella (37 genes). Pili, as the conductive appendages distributed on the surface of bacteria, can transfer electrons directly to the anode, the conductive pilus of electrogenic microorganisms is one of the important mechanisms of EET (Reguera et al. 2005; Lovley et al. 2006). In addition, pyoverdine contributes to the survival of microbes in nutrient-deficient soil (Ignacio et al. 2018).

Critical metabolic pathways

Genes were annotated against the KEGG databases to investigate the critical metabolic pathways involved in bioelectricity generation and bioelectrode catalysis in MFCs. For *P. stutzeri* S116, energy metabolism and a two-component system are the two essential functions in KEGG annotations (shown in Figure S5).

The respiratory chain on the membrane of *P. stutzeri* S116 is an important pathway for electron transport and energy production. Oxidative phosphorylation (ko00190, 36 genes) indicated that the strain S116 possessed an integrated electron transport chain. The critical enzymes including succinate dehydrogenase (EC:1.3.5.1), ubiquinol-cytochrome c reductase (EC:1.10.2.2) and cbb3-type cytochrome c oxidase (EC:7.1.1.9, cytochrome aa3) were detected, which are all annotated in COGs. In complex II, *sdhC* (K00241), *sdhD* (K00242), *sdhA* (K00239) and *sdhB* (K00240) encode cytochrome b, membrane anchor subunit, iron-sulfur subunit and flavoprotein subunit, respectively, where succinate is dehydrogenized into fumarate. Complex III primarily contains ubiquinol-cytochrome c reductase iron-sulfur subunit (EC:7.1.1.8), ubiquinol-cytochrome c reductase cytochrome b subunit (K00412) and ubiquinol-cytochrome c reductase cytochrome c1 subunit (K00413). The electrons are transported from complex III to cytochrome c oxidase (complex IV) via cytochrome c, where oxygen is reduced into H_2O and energy is generated. Nevertheless, annotated type 2 NADH dehydrogenase (K03885, EC:1.6.99.3) is involved in regulation rather than respiration (Howitt et al. 1999). Therefore, electron transport in *P. stutzeri* S116 forms a succinate pathway with high probability (Figure S6).

Generally, there are two oxidation pathways from thiosulfate to SO_4^{2-} or $S_4O_6^{2-}$ for SOB: (1) $S_2O_3^{2-}$ is oxidized to SO_4^{2-} by the Sox multienzyme complex (Fiedrich et al. 2005). (2) Thiosulfate dehydrogenase (EC:1.8.2.2, *tsdA*) catalyzes $S_2O_3^{2-}$ to $S_4O_6^{2-}$ (Brito et al. 2015). Simultaneously, the pathway of sulfur metabolism (ko00920, 34 genes) indicates that thiosulfate is catalyzed by thiosulfate sulfurtransferase

(EC:2.8.1.1) into sulfite. Moreover, the *sqr* gene encoding sulfide:quinone oxidoreductase (EC:1.8.5.4) was detected, which can oxidate H_2S into S_0.

Riboflavin can freely shuttle cell membranes and capture electrons from the respiratory chain, which plays an important role in EET. Riboflavin metabolism (ko00740 8 genes) for *P. stutzeri* indicates that ribulose 5-phosphate is metabolized into riboflavin. In addtion, riboflavin, as a redox active compound, is secreted by many bacteria (Abbas et al. 2011). COG0307 and COG0196 encoding riboflavin synthase and riboflavin kinase are annotated in COG, which are essential enzymes related to the biosynthesis of riboflavin.

Pilus are generally detected in gram-negative bacteria and closely related to bacterial activity, biofilm formation, surface adhesion, DNA acquisition and signal transduction (Reardon et al. 2013). Genes encoding type IV pilus-assembly proteins, such as *pilB*, *pilC*, *pilE*, *pilW*, *pilZ*, *pilV*, *pilO*, *pilM*, *pilN*, *pilQ*, *pilY*, *pilV* and *pilP*, were detected in the COG and KEGG databases. Two-component system (ko02020, 153 genes) for *P. stutzeri* involved in chemotaxis primarily includes twitching motility proteins encoded by genes such as *pilG*, *pilH*, *pilI*, *pilJ*, and *pilK*. Moreover, the redox signal is transmitted by the annotated critical sensor histidine kinase (EC:2.7.13.3, K15011) into an electron transfer system and aerobic respiration. Simultaneously, the system indicated that nitrate and nitrite were phosphorylated and transported to nitrate reductase, and finally entered the nitrogen metabolism pathway (ko00910, 36 genes). The predicted metabolic pathways in *P. stutzeri* were shown in Fig. 6.

Discussion

Pseudomonas is a typical electrogenic microorganism applied in bioanode MFCs (Arkatkar et al. 2021). However, for biocathode MFCs, few studies have described it comprehensively and completely. Here, the strain S116 exhibited excellent performance as a biocathode catalyst. The low Rct (11.8 Ω) values of biocathode indicates that S116 is a highly efficient catalyst between the biofilm and the cathode electrode. Moreover, the cost of biocathode MFCs are distinctly lower than abiotic MFCs (such as transition metal elements, Pt-coated metals, and ferricyanide). Simultaneously, biocathodes can improve MFCs sustainability due to consumption of electron mediator is solved (Bergel et al. 2005). In a word, *P. stutzeri* S116 is a promising electrogenic microorganism possessing bifunctional catalysis applied in MFCs.

Many genes encoding cytochrome c annotated for COG function analysis, which can form a complex extracellular electron transport network and realize the transmembrane transport of electrons (Li et al. 2018; Shelobolina et al. 2007; Orellana et al. 2013). Simultaneously, type IV pilus as “Nanowires” were detected. However, the truncated pilus protein (*pilA* encoding) was not founded in databases, which is closely related to the pilus with highly electrical conductivity (Campos et al. 2013). Redox mediators such as riboflavin can intercept electrons from the respiratory chain, and transfer them outside the cell membrane (Lovely 2012). Riboflavin metabolism pathway indicated 8 critical genes involved in riboflavin synthesis. The critical riboflavin synthase (EC:2.5.1.9) in the reaction process is detected, which catalyzes

the last step of riboflavin biosynthesis in microorganisms. Subsequently, riboflavin is synthesized into dimethyl-benzimidazole (entering porphyrin and chlorophyll metabolism) or FAD. In the VFDB, six genes (*phzF1*, *phzC1*, *phzG1*, *phzH*, *phzE*1 and *phzD*1) are responsible for phenazine biosynthesis. Phenazine secreted by *P. aeruginosa* is a heterocyclic compound containing nitrogen, which plays an important role in EET as a physiological electron transfer mediator of electricigens (Zee et al. 2009). Herein, the CV curve indicated that the definite reduction and oxidation peaks were detected in the range of -0.7 V~ 0 V (vs. Ag/AgCl electrode), which approaches the redox potential of phenazine and riboflavin (Zhang et al. 2011). Due to the lack of an intact *Sox* complex,thiosulfate oxidation probably performs the pathway where $S_2O_3^{2-}$ is catalyzed to $S_4O_6^{2-}$ by *tsdA*. However, the protein *tsdB* was not detected inS116, which is generally considered to the electronic acceptor in *Pseudomonas stutzeri* (Denkmann et al. 2012). The *tsdA* probably acts an electron acceptor to oxidize $S_2O_3^{2-}$ in some SOB.

The nitrogen metabolism pathway implies that *P. stutzeri* can treat wastewater containing nitrite. Nitrate can be reduced into nitrogen through denitrifying bacteria. The nitrogen metabolism pathway indicates that functional denitrification genes such as *nirS* (playing an important role in nitrite reduction), *norB*, *nosZ*, and *narG* (Chen et al. 2020) are detected in *P. stutzeri* S116 with denitrification. In addition, nitrate is metabolized into ammonia through dissimilatory nitrate reduction, and the annotated gene *nirBD* encodes nitrite reductase (EC:1.7.1.15) for nitrite reduction (Shi et al. 2019).

The study provided a promising bifunctional biocatalyst appiled in MFCs. Complete genome sequence of *Pseudomonas stutzeri* S116 and CV data represent the redox mediators secreted by *P. stutzeri* S116 were probably responsible for performance of MFCs. The critical genes and metabolic pathways involved in thiosulfate oxide and nitrate reduction were detected, which indicated that the strain can efficiently treat wastewater containing sulfide and nitrite.

Declarations

Acknowledgements

Not applicable.

Author contribution statement

CYZ, CDN conceived and de-signed the research. PL and YTH conducted the experiments. QL, ZHZ contributed new reagents or analytical tools. PL and JXW analyzed the data. PL wrote the manuscript. All authors read and approved the final manuscript.

Availability of data and materials

The data of this strain was uploaded as a bioproject to the National Center for Biotechnology Information (NCBI) database (PRJNA743140).

Funding

This work was financially supported by the the Zhoushan Science and Technology Bureau (project number 2016C41001), the Province Key Research and Development Program of Zhejiang (2021C02047), Key Laboratory of Cultivation and High-Value Utilization of Marine Organisms in Fujian Province (HXKJ2019095), College Students' Innovative Entrepreneurial Training Plan Program (202110340063).

Ethics approval and consent to participate

This article does not contain any studies that involve human participants or animals.

Consent for publication

Not applicable.

Competing interests

The authors declare no competing interests.

Author details

[1]School of Ocean Science and Technology, Zhejiang Ocean University, Zhoushan, Zhejiang 316022, China.[2]Fisheries Research Institute of Fujian Province, Xiamen 361013, China.

References

1. Abbas CA, Sibirny AA (2011) Genetic control of biosynthesis and transport of riboflavin and flavin nucleotides and construction of robust biotechnological producers. Microbiol. Mol Biol R 75:321–360. https://doi.org/10.1128/MMBR.00030-10
2. Ali N, Anam M, Yousaf S, Maleeha S, Bangash Z (2017) Characterization of the electric current generation potential of the *Pseudomonas aeruginosa* using glucose, fructose, and sucrose in double chamber microbial fuel cell. Iran J Biotechnol 15:216–223. https://doi.org/10.15171/ijb.1608
3. Altschul SF, Madden TL, Schäffer AA (1997) Gapped BLAST and PSI-BLAST: a new generation of protein database search programs. Nucleic Acids Res 25:3389–3402. https://doi.org/10.1093/nar/25.17.3389
4. Arkatkarab A, Mungray KA, Sharma P (2021) Study of electrochemical activity zone of Pseudomonas aeruginosa in microbial fuel cell. Process Biochem 101:213–217. https://doi.org/10.1016/j.procbio.2020.11.020
5. Ashburner M, Ball CA, Blake JA (2000) Gene Ontology: tool for the unification of biology. Nat Genet 25:25–29. https://doi.org/10.1038/75556
6. Boeckmann B, Bairoch A, Apweiler R (2003) The SWISS-PROT protein knowledgebase and its supplement TrEMBL in 2003. Nucleic Acids Res 31:365–370. https://doi.org/10.1093/nar/gkg095
7. Bosire EM, Blank LM, Rosenbaum, MA (2016) Strain-and substrate-dependent redox mediator and electricity production by *Pseudomonas aeruginosa*. Appl Environ Microb 82:5026–5038.

https://doi.org/10.1128/AEM.01342-16

8. Boobalan T, Samsudeen N, James O, Ebenezer S (2019) Comparative study on *Cronobacter sakazakii* and *Pseudomonas otitidis* isolated from septic tank wastewater in microbial fuel cell for bioelectricity generation. Fuel 248:47–55. https://doi.org/10.1016/j.fuel.2019.03.060
9. Brito, JA, Denkmann K, Pereira IAC, Archer M, Dahl C (2015) Thiosulfate dehydrogenase (TsdA) from *Allochromatium vinosum*: structural andfunctional insights into thiosulfate oxidation. J Biol Chem 290:9222–9238. https://doi.org/10.1074/jbc.M114.623397
10. Brutinel ED, Gralnick JA (2012) Shuttling happens: soluble flavin mediators of extracellular electron transfer in *Shewanella*. App Microbiol Biot 93:41–48. https://doi.org/10.1007/s00253-011-3653-0
11. Chadwick GL, Jim F, Gralnick JA, Bond DR, Orphan VJ (2019) NanoSIMS imaging reveals metabolic stratification within current-producing biofilms. PNAS 116:20716–20724. https://doi.org/10.1073/pnas.1912498116
12. Cai XH, Ch YS, Mao JJ (2020) Identifying the proton loading site cluster in the ba3 cytochrome c oxidase that loads and traps protons. BBA Bioenergetics 1861:148239–148253. https://doi.org/10.1016/j.bbabio.2020.148239
13. Campos M, Cisneros DA, Nivaskumar M (2013) The type II secretion system - a dynamic fiber assembly nanomachine. Res Microbiol 164:545–555. https://doi.org/10.1016/j.resmic.2013.03.013
14. Cao YJ, Mu H, Liu W, Zhang R, Guo J, Xian M, Liu H (2019) Electricigens in the anode of microbial fuel cells: pure cultures versus mixed communities. Microb Cell Fact 18:39–53. https://doi.org/10.1186/s12934-019-1087-z
15. Chen QR, Fan JF, Ming HX, Su J, Wang Y, Wang B (2020) Effects of environmental factors on denitrifying bacteria and functional genes in sediments of Bohai Sea, China. Mar Pollut Bull 160:111621–111632. https://doi.org/10.1016/j.marpolbul.2020.111621
16. Clauwaert P, Ha DVD, Boon N, Verbeken K, Rabaey K, Verstraete W (2007) Open air biocathode enables effective electricity generation with microbial fuel cells. Environ Sci Technol 41:7564–7569. https://doi.org/10.1021/es0709831
17. Denkmann K, Grein F, Zigann R, Siemen A, Bergmann J, van Helmont S, Nicolai A, Pereira IAC, Dahl C (2012) Thiosulfate dehydrogenase: a widespread unusual acidophilic c-type cytochrome. Environ Microbiol 14:2673–2688. https://doi.org/10.1111/j.1462-2920.2012.02820.x
18. Feng Y, Yang Q, Wang X, Logan BE (2010) Treatment of carbon fiber brush anodes for improving power generation in air–cathode microbial fuel cells. J Power Sources 195:1841–1844. https://doi.org/10.1016/j.jpowsour.2009.10.030
19. Fiedrich CG, Bardischewsky F, Rother D, Quentmeier A, Fischer J (2005) Prokaryotic sulfur oxidation. Curr Opin Microbiol 8:253–259. https://doi.org/10.1016/j.mib.2005.04.005
20. Hassan H, Jin B, Donner E (2018) Microbial community and bioelectrochemical activities in MFC for degrading phenol and producing electricity: Microbial consortia could make differences. Chem Eng J 332:647–657. https://doi.org/10.1016/j.cej.2017.09.114

21. Herbold CW, Lee CK, Mcdonald IR, Cary SC (2014) Evidence of global-scaleaeolian dispersal and endemism in isolated geothermal microbial communities of Antarctica. Nat Commun 5:3875–3884. https://doi.org/10.1038/ncomms4875
22. Holmes DE, Bond DR, Olneill RA (2004) Microbial communities associated with electrodes harvesting electricity from a variety of aquatic sediments. Microb Ecol 48:178–190. https://doi.org/10.1007/s00248-003-0004-4
23. Howitt CA, Udall PK, Vermaas WF (1999) Type 2 NADH dehydrogenases in the *cyanobacterium Synechocystis* sp. strain PCC 6803 are involved in regulation rather than respiration. Bacteriol 181:3994–4003. https://doi.org/10.1128/jb.181.13.3994-4003.1999
24. Hwang JH, Kim KY, Eleazer PR, Lee WH (2019) Surfactant addition to enhance bioavailability of bilge water in single chamber microbial fuel cells (MFCs). J Hazard Mater 368:732–738. https://doi.org/10.1016/j.jhazmat.2019.02.007
25. Hyatt D, Chen GL, LoCascio PF (2010) Prodigal: prokaryotic gene recognition and translation initiation site identification. BMC Bioinformatics 11:119–129. https://doi.org/10.1186/1471-2105-11-119
26. Ignacio, D, Ester S, Jimena A, Ruiz JA (2018) Contribution of the Siderophores Pyoverdine and Enantio-Pyochelin to Fitness in Soil of *Pseudomonas protegens* Pf-5. Curr Microbiol 75:1560–1565. https://doi.org/10.1007/s00284-018-1560-7
27. Kanehisa M, Goto S, Kawashima S (2004) The KEGG resource for deciphering the genome. Nucleic Acids Res 32: 277–280. https://doi.org/10.1093/nar/gkh063
28. Kelly DP, Shergill JK, Lu WP, Wood AP (1997) Oxidative metabolism of inorganic sulfur compounds by bacteria. Anton Leeuw Int J G 71:95–107. https:// doi.org/10.1023/A:1000135707181
29. Koren S, Walenz BP, Berlin K (2017) Canu: scalable and accurate long-read assembly via adaptive k-mer weighting and repeat separation. Genome Res 116:1–36. https://doi.org/10.1101/gr.215087.116
30. Kumar R, Singh L, Zularisam AW (2016) Exoelectrogens: recent advances in molecular drivers involved in extracellular electron transfer and strategies used to improve it for microbial fuel cell applications. Renew Sust Energ Rev 56:1322–1336. https://doi.org/10.1016/j.rser.2015.12.029
31. Li M, Zhou MH, Tian XY, Tan CL, MaDaniel CT, Hassett DJ, Gu TY (2018) Microbial fuel cell (MFC) power performance improvement through enhanced microbial electrogenicity. Biotechnol Adv 36:1316–1327. https://doi.org/10.1016/j.biotechadv.2018.04.010
32. Logan BE, Rossi R, Ragab A, Saikaly PE (2019) Electroactive microorganisms in bioelectrochemical systems. Nat Rev Microbiol 17:307–319. https://doi.org/10.1038/s41579-019-0173-x
33. Logan BE (2009) Exoelectrogenic bacteria that power microbial fuel cells. Nat Rev Microbiol 7:375–381. https://doi.org/10.1038/nrmicro2113
34. Lovley DR (2011) Live wires: direct extracellular electron exchange for bioenergy and the bioremediation of energy-related contamination. Energ. Environ Sci 4:4896–4906. https://doi.org/10.1039/c1ee02229f

35. Lovley DR (2006) Bug juice: harvesting electricity with microorganisms. Nat Rev Microbiol 4:497–508. https://doi.org/10.1038/nrmicro1442
36. Lovely DR (2012) Electromicrobiology. Annu Rev Microbiol 66:391–409. https://10.1371/journal.pone.0091484
37. Lowe TM, Eddy SR (1997) tRNAscan-SE: a program for improved detection of transfer RNAgenes in genomic sequence. Nucleic Acids Res 25:955–964. https://doi.org/10.1093/nar/25.5.955
38. Marshall CW, LaBelle EV, May HD (2013) Production of fuels and chemicals from waste by microbiomes. Curr Opin Biotech 24:391–397. https://doi.org/10.1016/j.copbio.2013.03.016
39. Mubaroka MZ, Winarko R, Chaeruna SK, Rizkic IN, Ichlas ZT (2017) Improving gold recovery from refractory gold ores through biooxidation using iron-sulfur oxidizing /sulfur-oxidizing mixotrophic bacteria. Hydrometallurgy 168: 69–75. https://doi.org/10.1016/j.hydromet.2016.10.018
40. Omri I, Aouidi F, Bouallagui H, Godon JJ, Hamdi M (2013) Performance study of biofilter developed to treat H_2S from wastewater odour. Saudi J Biol Sci 20:169–176. https://doi.org/10.1016/j.sjbs.2013.01.005
41. Orellana R, Leavitt JJ, Comolli LR, Csencsits R, Lovley DR (2013) U(VI) reduction by diverse outer surface c-type cytochromes of *Geobacter sulfurreducens*. Appl Environ Microbiol 79:6369–6374. https://doi.org/10.1128/AEM.02551-13
42. Park DH, Zeikus JG (1999) Utilization of electrically reduced neutral red by Actinobacillus succinogenes: Physiological function of neutral red in membrane-driven fumarate reduction and energy conservation. Bacteriology 181:2403–2410. https://doi.org/10.1128/JB.181.8.2403-2410.1999
43. Pokorna D, Zabranska J (2015) Sulfur-oxidizing bacteria in environmental technology. Biotechnol Adv 33:1246–1259. https:// doi.org/10.1016/j.biotechadv.2015.02.007
44. Prenafeta-Boldu FX, Rojo N, Gallastegui G, Guivernau M, Vinas M, Elias A (2014) Role of *Thiobacillus thioparus* in the biodegradation of carbon disulfide in a biofilter packed with a recycled organic pelletized material. Biodegradation 25:557–568. https:// doi.org/10.1007/s10532-014-9681-6
45. Quijano G, Figueroa GI, Buitron G (2018) Fully aerobic two-step desulfurization process for purification of highly H_2S-laden biogas. J Chem Technol Biot 93:3553–3561. https://doi.org/10.1016/j.sjbs.2013.01.005
46. Reardon PN, Mueller KT (2013) Structure of the type IV a major pilin from the electrically conductive bacterial nanowires of *Geobacter sulfurreducens*. J Biol Chem 288:29260–29266. https://doi.org/10.1074/jbc.M113.498527
47. Reguera G, Mccarthy KD, Mehta T (2005) Extracellular electron transfer via microbial nanowires. Nature 435:1098–1101. https://doi.org/10.1038/nature03661
48. Samsudeen N, Radhakrishnan TK, Matheswaran M (2016) Effect of isolated bacterial strains from distillery wastewater on power generation in microbial fuel cell. Process Biochem 51:1876–1884. https://doi.org/10.1016/j.procbio.2016.06.007

49. San-Valero P, Penya-Roja JM, Alvarez HFJ, Buitron G, Gabaldon C, Quijano G (2019) Fully aerobic bioscrubber for the desulfurization of H_2S-rich biogas. Fuel 24:884–891. https://doi.org/10.1016/j.fuel.2018.12.098
50. Saranya N, Jayapriya J (2018) Improved performance of *Pseudomonas aeruginosa* catalyzed MFCs with graphite/polyester composite electrodes doped with metal ions for azo dye degradation. Chem Eng J 343:258–26. https://doi.org/10.1016/j.cej.2018.02.123
51. Saratale GD, Saratale RG, Shahid MK, Zhen GY, Kumar G, Shin HS, Choi YG, Kim SH (2017) A comprehensive overview on electro-active biofilms, role of exo-electrogens and their microbial niches in microbial fuel cells (MFCs). Chemosphere 178:534–547. https://doi.org/10.1016/j.chemosphere.2017.03.066
52. Sedky HA, Hassana AG, Woo K (2019) Real-time monitoring of water quality of stream water using sulfur-oxidizing bacteria as bio-indicator. Chemosphere 223:58–63. https://doi.org/10.1016/j.chemosphere.2019.01.089
53. Shelobolina ES, Coppi MV, Korenevsky AA, Didonato LN, Sullivan SA, Konishi H, Xu H, Leang, C, Butler JE, Kim, BC (2007) Importance of c-Type cytochromes for U(VI) reduction by *Geobacter sulfurreducens*. BMC Microbiol 7: 16–30. https://doi.org/10.1186/1471-2180-7-16
54. Shi JW, Zang XN, Cong XM (2019) Cloning of nitrite reductase gene from *Haematococcus pluvialis* and transcription and enzymatic activity analysis at different nitrate and phosphorus concentration. Gene 697:123–130. https://doi.org/10.1016/j.gene.2019.01.042
55. Tatusov RL, Galperin MY, Natale DA (2000) The COG database: a tool for genome-scaleanalysis of protein functions and evolution. Nucleic Acids Res 28:33–36. https://doi.org/10.1093/nar/28.1.33
56. Wu X, Tong F, Yong X, Zhou J, Zhang L, Jia H, Wei P (2016) Effect of NaX zeolite-modified graphite felts on hexavalent chromium removal in biocathode microbial fuel cells. J Hazard Mater 308:303-311. https://doi.org/10.1016/j.jhazmat.2016.01.070
57. Xi L, Wang SW, Xu AM (2019) Biological synthesis of high-conductive pili in aerobic bacterium *Pseudomonas aeruginosa*. Appl Microbiol Biot 103:1535-1544. https://doi.org/10.1007/s00253-018-9484-5
58. Xie X, Ye M, Hu L, Liu N, McDonough JR, Chen W, Alshareef HN, Criddle CS, Cui Y (2012) Carbon nanotube-coated macroporous sponge for microbial fuel cell electrodes. Energ Environ Sci 5:5265–5270. https://doi.org/10.1039/C1EE02122B
59. Xu HD, Quan XC (2016) Anode modification with peptide nanotubes encapsulating riboflavin enhanced power generation in microbial fuel cells. Int J Hydrogen Energ 41:1966–1973. https://doi.org/10.1016/j.ijhydene.2015.11.124
60. Zee FPVD, Cervantes FJ (2009) Impact and application of electron shuttles on the redox (bio)transformation of contaminants: A review. Biotechnol Adv 27:256–277. https://doi.org/10.1016/j.biotechadv.2009.01.004
61. Zhang M, Ma Z, Zhao N, Zhang K, Song H (2019) Increased power generation from cylindrical microbial fuel cell inoculated with *P. aeruginosa*. Biosens Bioelectron 141:111394–111399.

https://doi.org/10.1016/j.bios.2019.111394

62. Zhang TT, Zhang LX, Su WT (2011) The direct electrocatalysis of phenazine-1-carboxylic acid excreted by *Pseudomonas alcaliphila* under alkaline condition in microbial fuel cells. Bioresource Technol 102:7099–7102. https://doi.org/10.1016/j.biortech.2011.04.093
63. Zhou Q, Liang H, Yang S, Jiang X (2015) The removal of hydrogen sulfide from biogas in a microaerobic biotrickling filter using polypropylene carrier as packing material. Appl Biochem Biotech 175:3763–3777. https:// doi.org/10.1007/s12010-015-1545-y

Figures

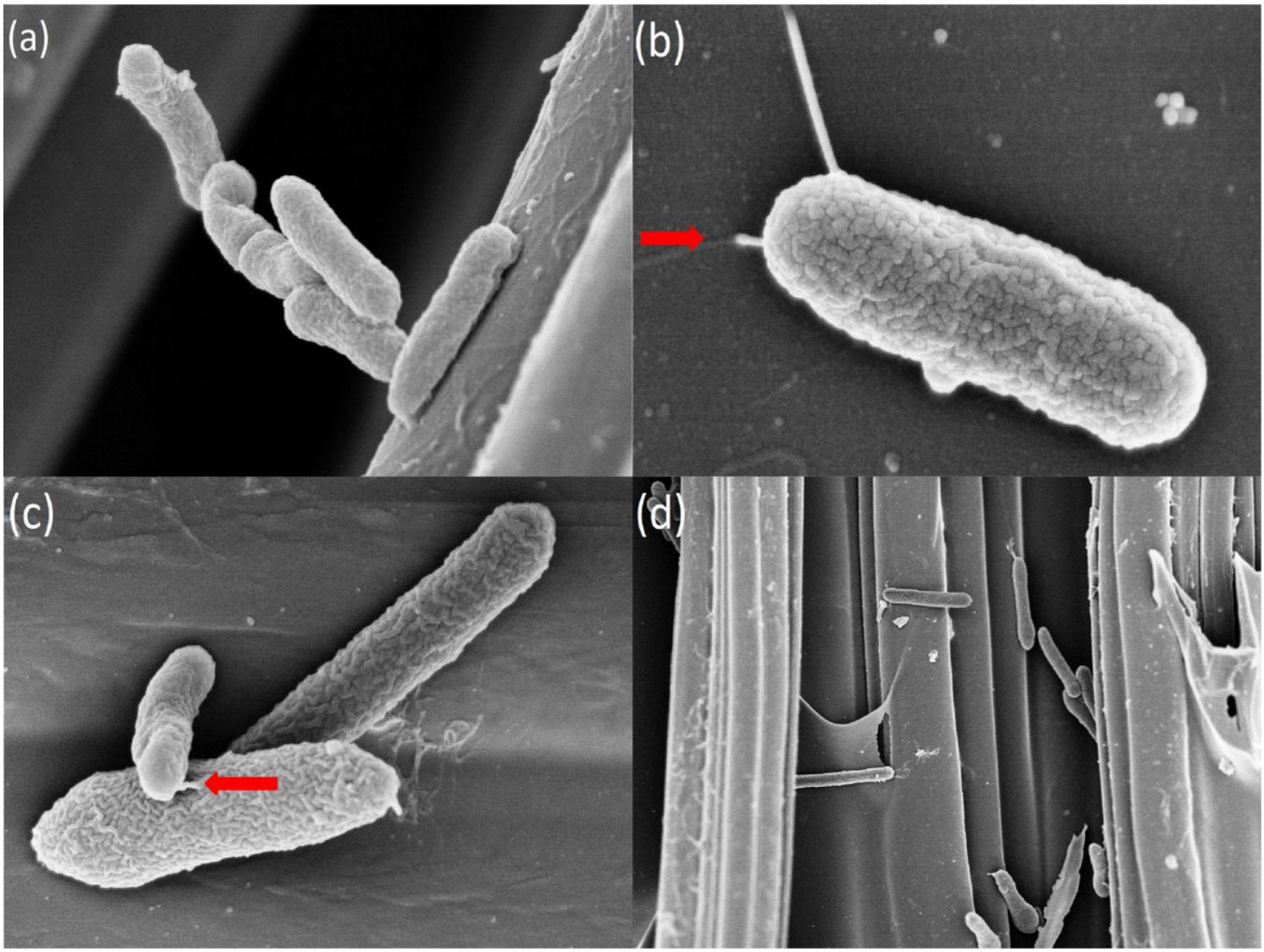

Figure 1

SEM of microorganism on bare carbon fiber (red arrow: flagella).

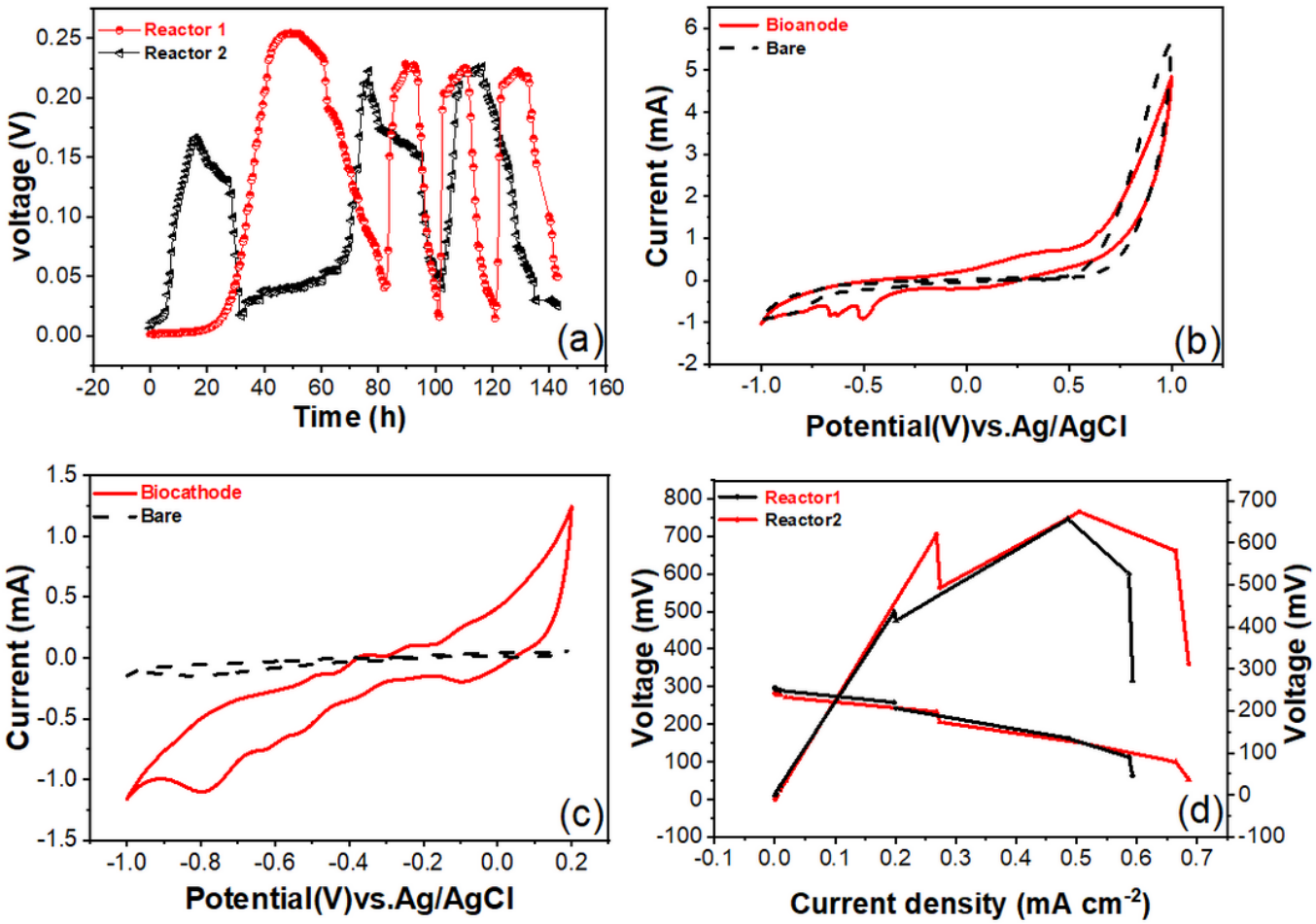

Figure 2

(a)Voltage output , (b) (c) Cyclic voltammogram (CV) of the bioanode and the biocathode, (d) power density and polarization curves of MFC.

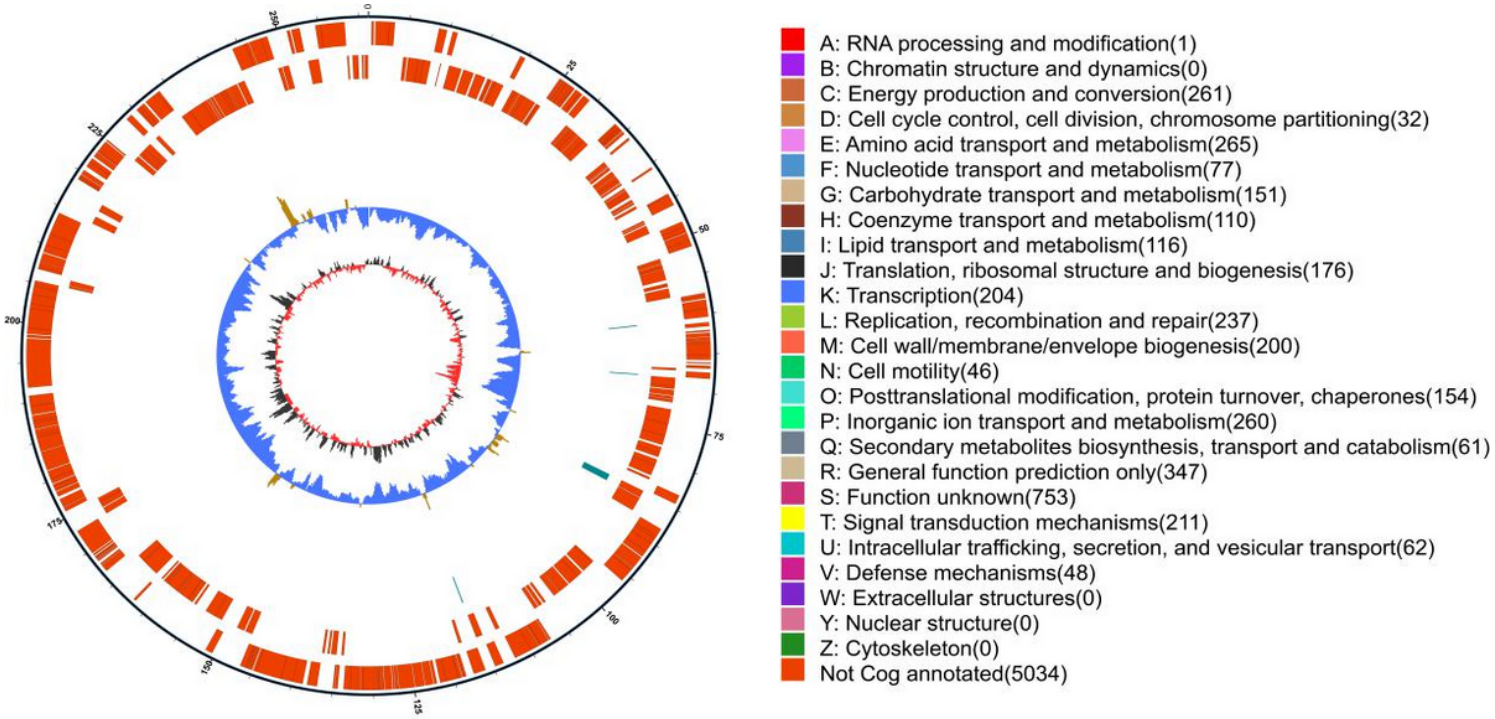

Figure 3

Schematic of the complete genome of *P. stutzeri* S116 isolated from marine activated sludge samples. The first circle (outermost) indicates genomic numbers, with each tick representing 5 kb; genes on forward and reverse chains with different colors based on COG categories are represented at the second and third circles; repetitive sequences (fourth circle); tRNA with bule and rRNA with purple (fifth circle); GC skew (sixth circle). The light yellow region indicates that the GC content is higher than the average in the genome; nevertheless, the bule region represents the opposite. The dark gray region represents G content greater than C, and the red region represents C content greater than G.

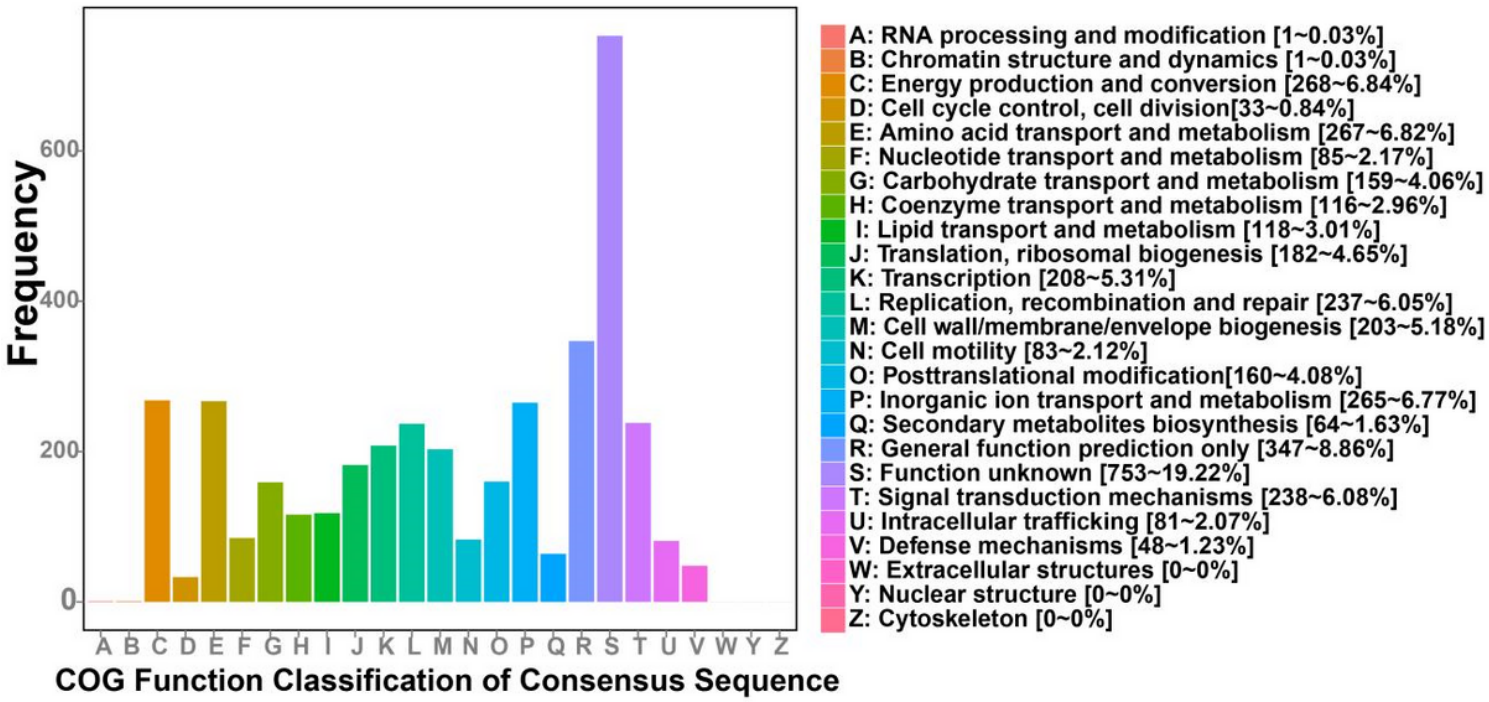

Figure 4

Functional categories of *P. stutzeri* S116 annotated by clusters of orthologous groups of proteins (COGs).

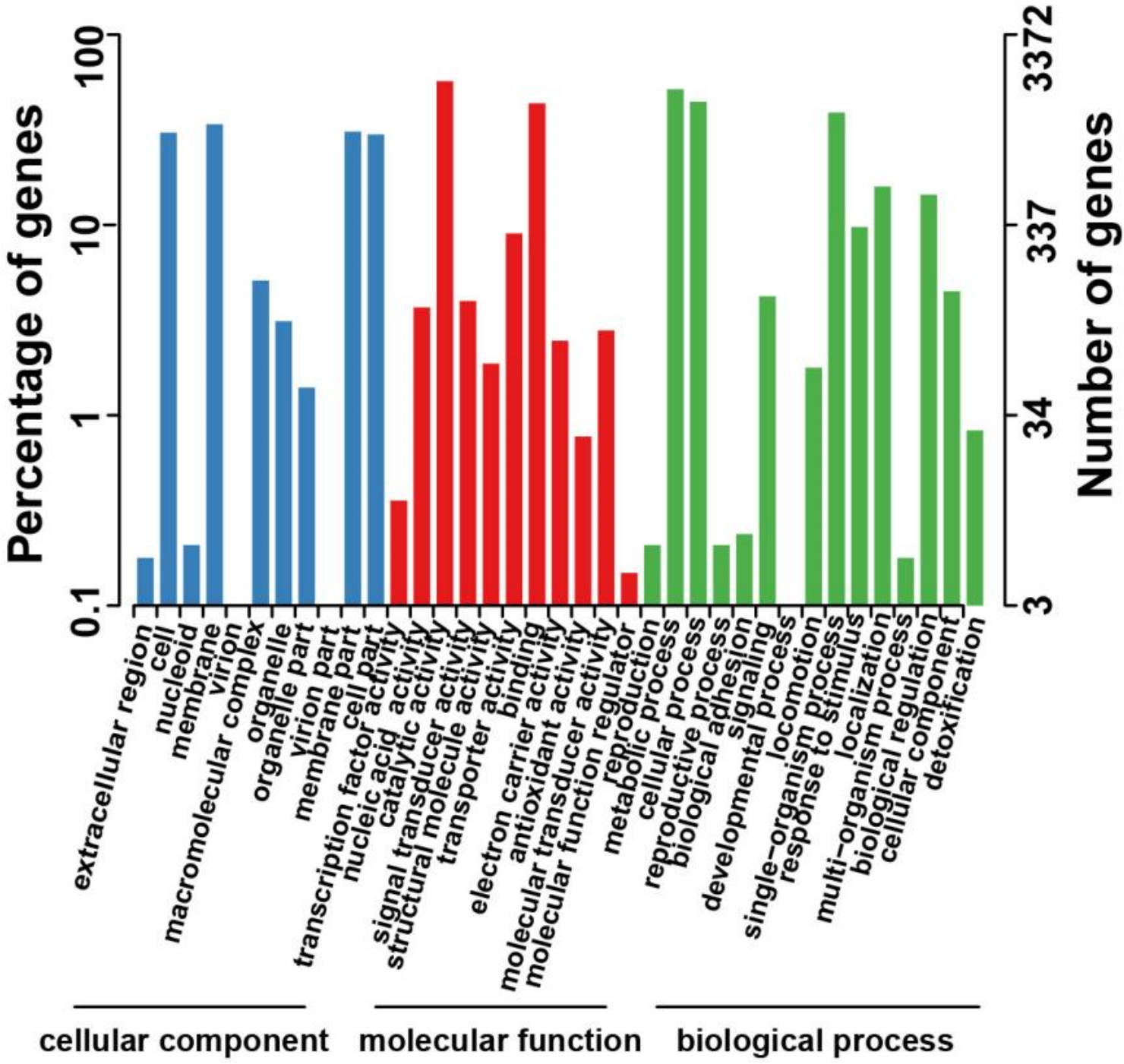

Figure 5

GO Classification for *P. stutzeri* S116 isolated from marine activated sludge. The chart shows the enriched genes with secondary-level functions in all genes against GO.

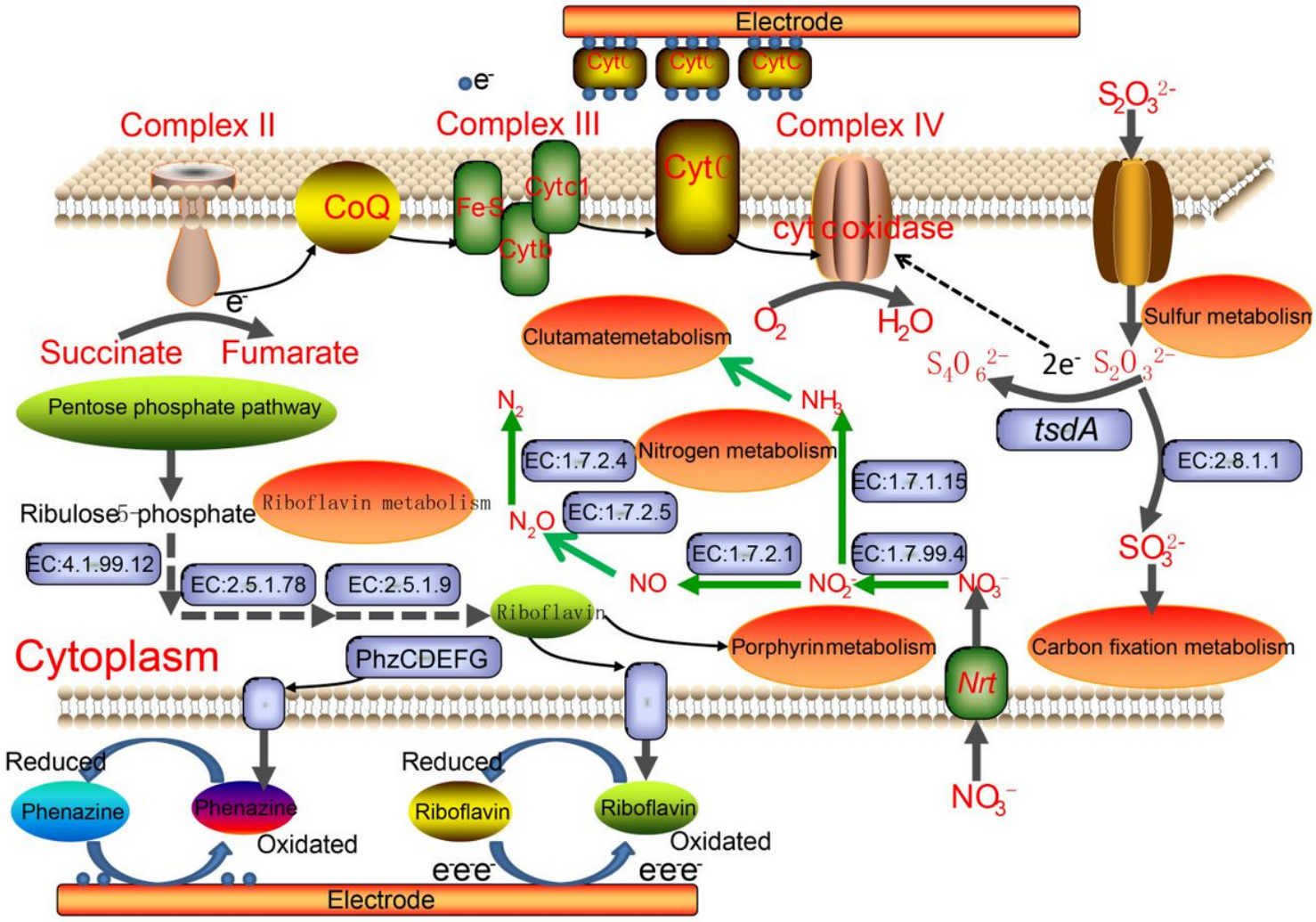

Figure 6

Metabolic pathways for *P. stutzeri* S116 involved the electron respiratory chain, nitrate reduction pathway, thiosulfate oxidation pathway, riboflavin metabolism and the predicted EET pathway between the electronic mediators and the electrodes.

Supplementary Files

This is a list of supplementary files associated with this preprint. Click to download.

- Supplementarymaterials.pdf